Is the efficacy of satellite-based inversion of SO_2 emission model dependent?

Nan Li [1], Keqin Tang [1], Yi Wang [2], Jun Wang [2], Weihang Feng [1], Haoran Zhang [1], Hong Liao [1], Jianlin Hu [1], Xin Long [3], Chong Shi [4], Xiaoli Su [5]

[1]Jiangsu Key Laboratory of Atmospheric Environment Monitoring and Pollution Control, Jiangsu Collaborative Innovation Center of Atmospheric Environment and Equipment Technology, School of Environmental Science and Engineering, Nanjing University of Information Science & Technology, Nanjing, 210044, China

[2]Center of Global and Regional Environmental Research, Department of Chemical and Biochemical Engineering, University of Iowa, Iowa City, Iowa, USA

[3]School of Environment Science and Engineering, Southern University of Science and Technology, Shenzhen, 518055, China

[4]Japan Aerospace Exploration Agency, Earth Observation Research Center, 2-1-1, Sengen, Tsukuba, Ibaraki, Japan

[5]Key Lab of Aerosol Chemistry & Physics, SKLLQG, Institute of Earth Environment, Chinese Academy of Sciences, Xi'an, 710061, China

Correspondence to:

Nan Li, linan@nuist.edu.cn

Yi Wang, yi-wang-4@uiowa.edu

Jun Wang, jun-wang-1@uiowa.edu

Table S1. Model settings in different simulation scenarios

	Meteorology field	Gaseous chemistry	Aerosol chemistry	Dry and wet depositions
GEOS-Chem	GEOS-5	NOx-Ox-Hydrocarbon-Aerosol mechanism Explicit mechanism, including 116 species and 311 reactions. The globchem.dat file in GEOS-Chem adjoint v35d run directory	RPMARES 3 modes: aitken, accumulation and coarse Binkowski et al., 2003	Wang et al., 1998 Wesely, 1989 Liu et al., 2001
WRF-Chem	Online WRF	RADM2 Lumped mechanism, including 63 species and 145 reactions, VOC species are categorized based on their reactivity with OH radical Stockwell et al., 1990	SORGAM 3 modes: aitken, accumulation and coarse Schell et al., 2001	Easter et al., 2004 Zaveri et al., 2005
	Online WRF	SAPRC99 Lumped mechanism, including 74 species and 211 reactions, VOC species are categorized based on their reactivity with OH radical Carter et al., 2000a Carter et al., 2000b	MOSAIC 8-bin: from 0.04 □m to 10 □m Zaveri et al., 2008	Easter et al., 2004 Zaveri et al., 2005
	Online WRF	SAPRC99 Lumped mechanism, including 74 species and 211 reactions, VOC species are categorized based on their reactivity with OH radical Carter et al., 2000a Carter et al., 2000b	MOSAIC + heterogeneous sulfate 8-bin: from 0.04 □m to 10 □m Zaveri et al., 2008 Wang et al., 2016	Easter et al., 2004 Zaveri et al., 2005
CMAQ	Offline WRF	SAPRC11 Lumped mechanism, including 139 species and 351 reactions, VOC species are categorized based on their reactivity with OH radical Carter and Heo, 2012	AERO6 3 modes: aitken, accumulation and coarse Carlton et al., 2010	Foley et al., 2010

Table S2. Observed and simulated vertical column SO_2 (DU), surface SO_2 (ppb) and AOD.

	Observation	Prior				Posterior			
		WRF-Chem RADM2	WRF-Chem SAPRC99	WRF-Chem SAPRC99-het	CMAQ SAPRC11	WRF-Chem RADM2	WRF-Chem SAPRC99	WRF-Chem SAPRC99-het	CMAQ SAPRC11
Vertical column SO_2									
Jan	0.30	1.27	1.20	1.09	0.92	0.51	0.47	0.42	0.48
Apr	0.19	0.74	0.65	0.61	0.82	0.34	0.29	0.27	0.41
Jul	0.14	0.51	0.50	0.50	0.75	0.23	0.23	0.22	0.32
Oct	0.22	0.86	0.79	0.73	0.87	0.44	0.37	0.35	0.44
Annual	0.21	0.84	0.79	0.73	0.84	0.38	0.34	0.31	0.41
Surface SO_2									
Jan	22.2	33.7	34.2	33.1	40.3	13.0	13.0	12.6	20.7
Apr	12.9	21.6	21.7	21.2	31.5	9.9	9.8	9.6	13.0
Jul	9.2	21.5	20.1	20.6	23.2	10.1	9.6	9.5	12.1
Oct	12.7	26.3	26.0	25.4	36.4	12.1	11.9	11.7	17.1
Annual	14.3	25.8	25.5	25.1	32.9	11.3	11.1	10.8	15.7
AOD									
Jan	0.27	0.30	0.30	0.30	0.33	0.29	0.29	0.30	0.33
Apr	0.51	0.56	0.56	0.57	0.50	0.54	0.55	0.56	0.49
Jul	0.36	0.45	0.36	0.39	0.44	0.41	0.35	0.36	0.41
Oct	0.27	0.31	0.33	0.34	0.35	0.30	0.32	0.33	0.34
Annual	0.35	0.40	0.39	0.40	0.40	0.39	0.38	0.39	0.39

Table S3. Correlations of spatial distribution between GEOS-Chem result and other model results using prior SO_2 emissions.

	WRF-Chen RADM2	WRF-Chem SAPRC99	WRF-Chem SAPRC99-het	CMAQ SAPRC11
Vertical column SO_2				
GEOS-Chem	0.84	0.82	0.82	0.82
Surface SO_2				
GEOS-Chem	0.67	0.66	0.66	0.81

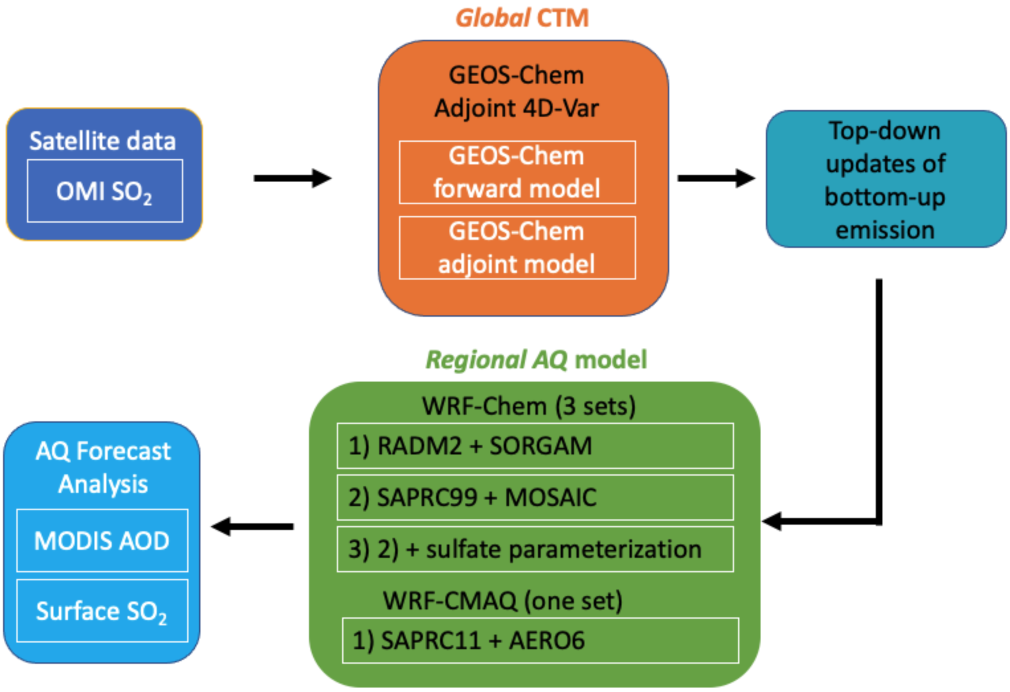

Figure S1. Framework of this study showing that the DA is conducted in one host model (GEOS-Chem) and the efficacy of the resultant top-down emissions are evaluated by two regional models that are different from the DA host model, WRF-Chem and WRF-CMAQ; for WRF-Chem, the evaluations are further conducted by using three sets of different chemistry mechanism.

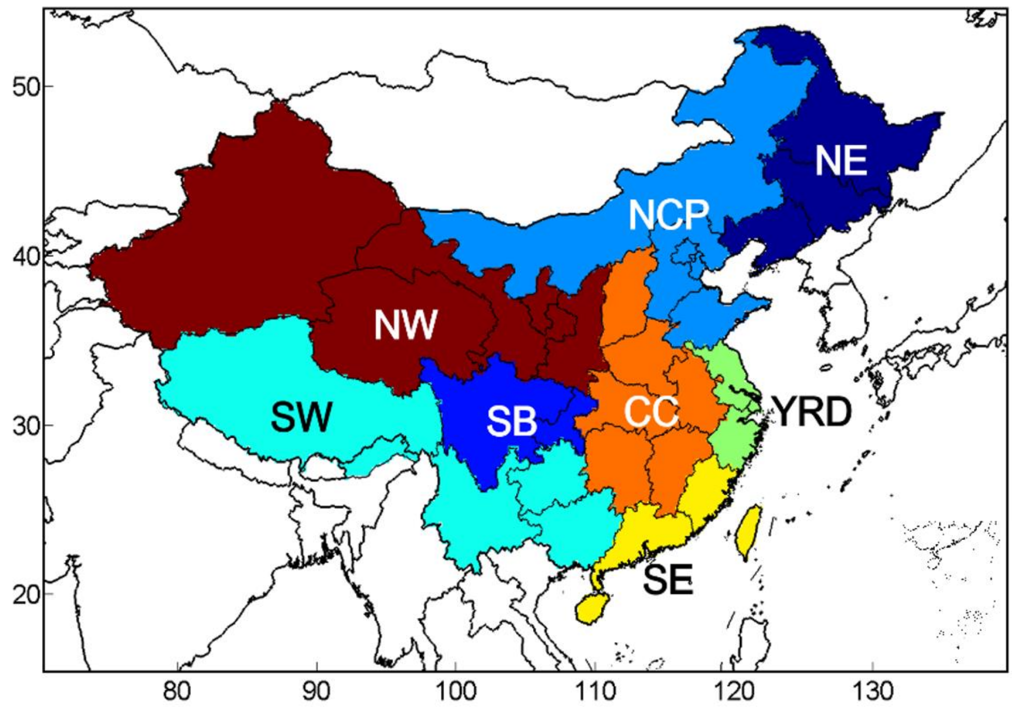

Figure S2. The model domain and region settings, including the Sichuan basin (SB), North China Plain (NCP), Central China (CC), Yangtze River Delta (YRD), Northwest China (NW), Northeast China (NE), Southwest China (SW), and Southeast China (SE).

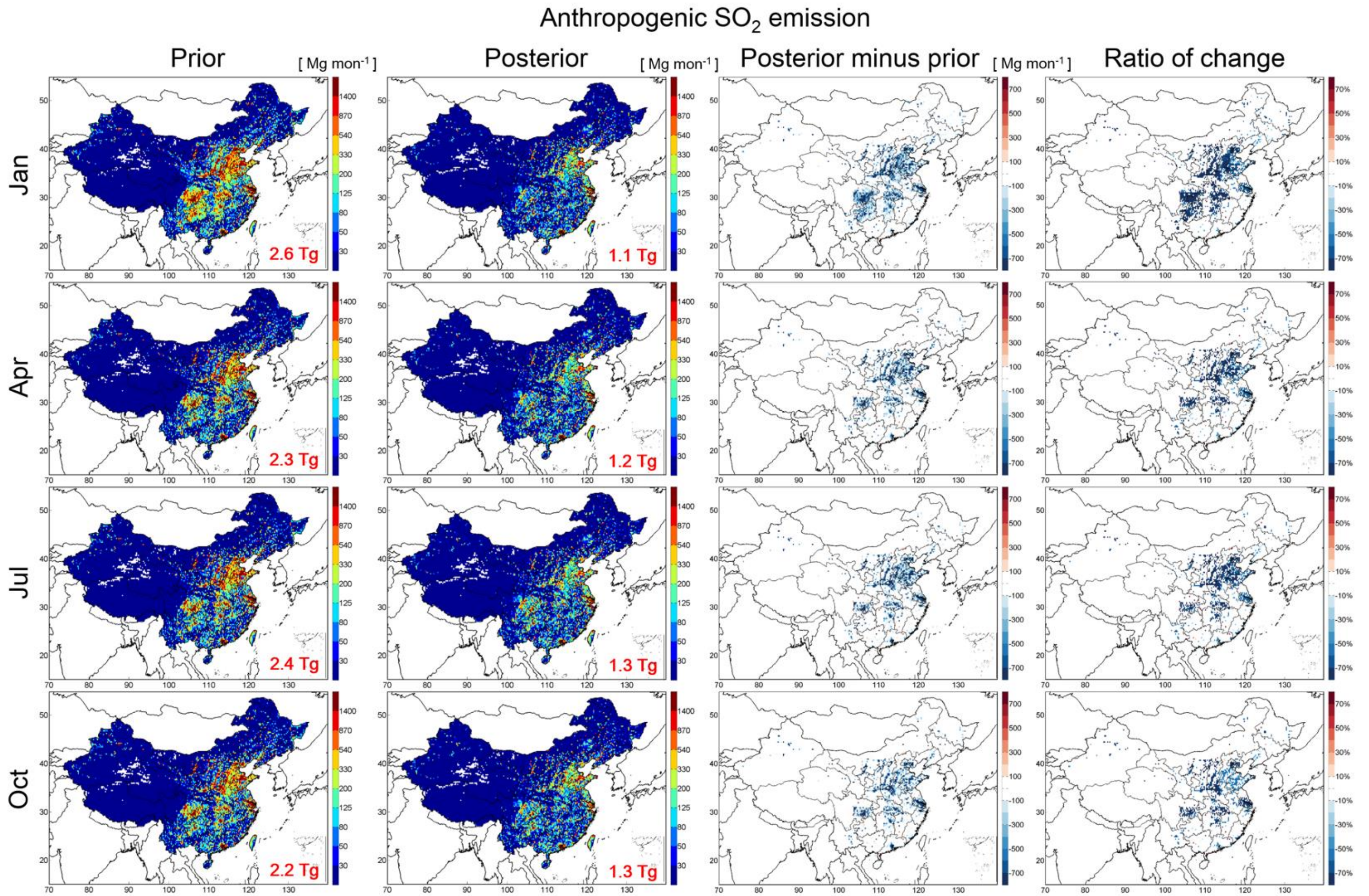

Figure S3. Monthly SO_2 emissions in 2009. The prior emission is from MEIC emission inventory, and the posterior emission is the satellite-constrained SO_2 emission using GEOS-Chem adjoint model. Regional emission totals are shown inset in red. The ratios of emission differences are shown in the grids where the differences are larger than 10 Mg mon^{-1}.

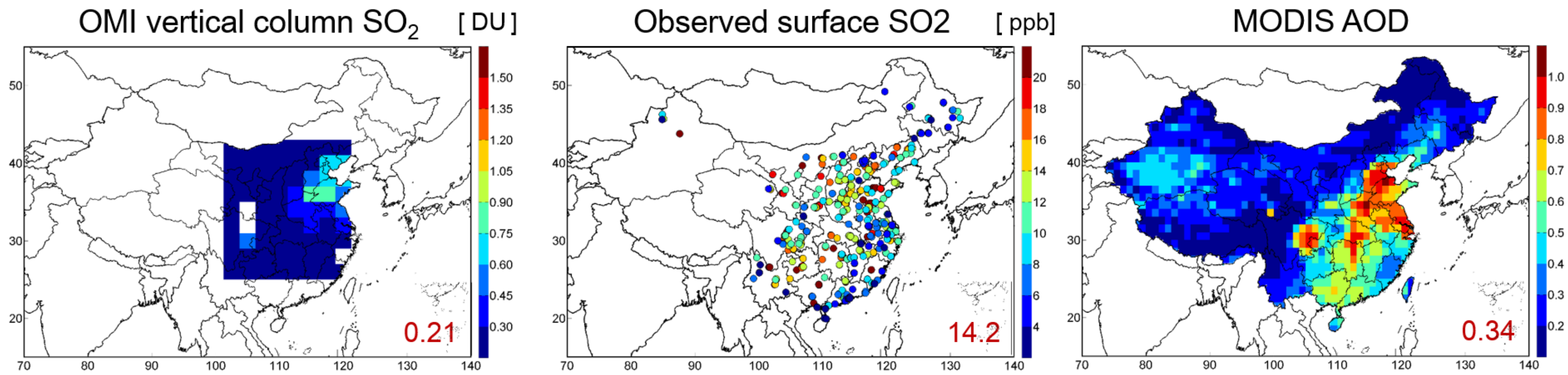

Figure S4. Annual vertical column SO_2 (DU) from OMI, surface SO_2 concentration from MEP observation network, and AOD from MODIS averaged for 2009.

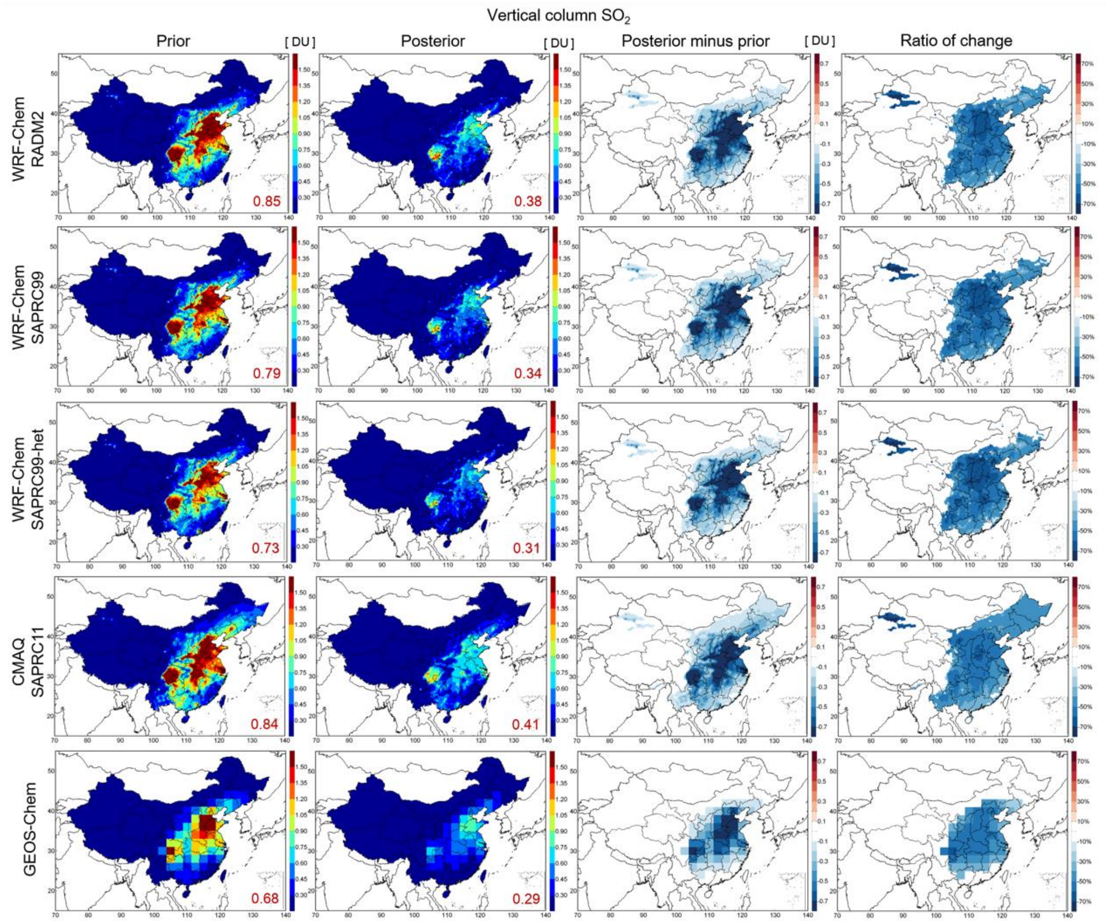

Figure S5. Annual vertical column SO_2 (DU) in China averaged for 2009. The left two columns are from prior and posterior simulations using different models and mechanisms and the right two columns are the differences between prior and posterior results. The ratios of differences are shown in the grids where the differences are larger than 0.1 DU.

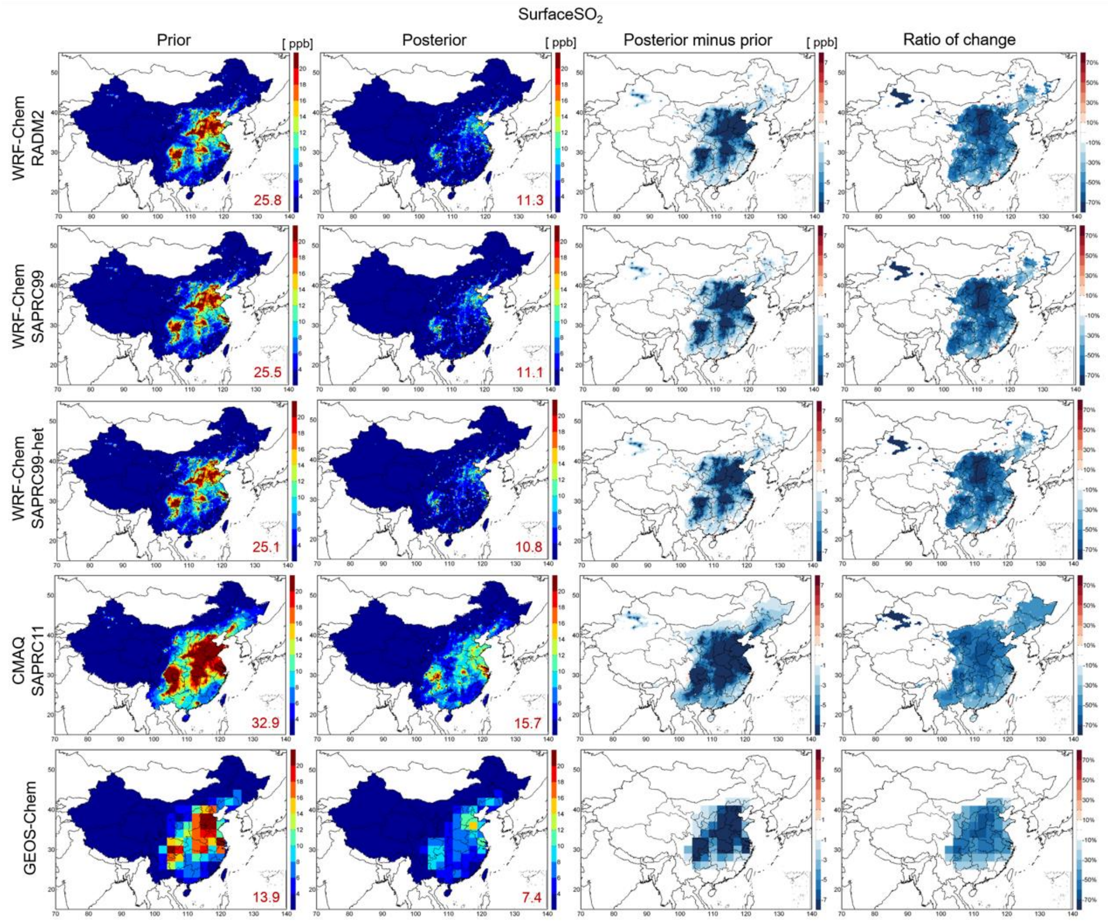

Figure S6. Annual surface SO_2 (ppb) in China averaged for 2009. The left two columns are from prior and posterior simulations using different models and mechanisms, and the right two columns are the differences between prior and posterior results. The ratios of differences are shown in the grids where the differences are larger than 1 ppb.

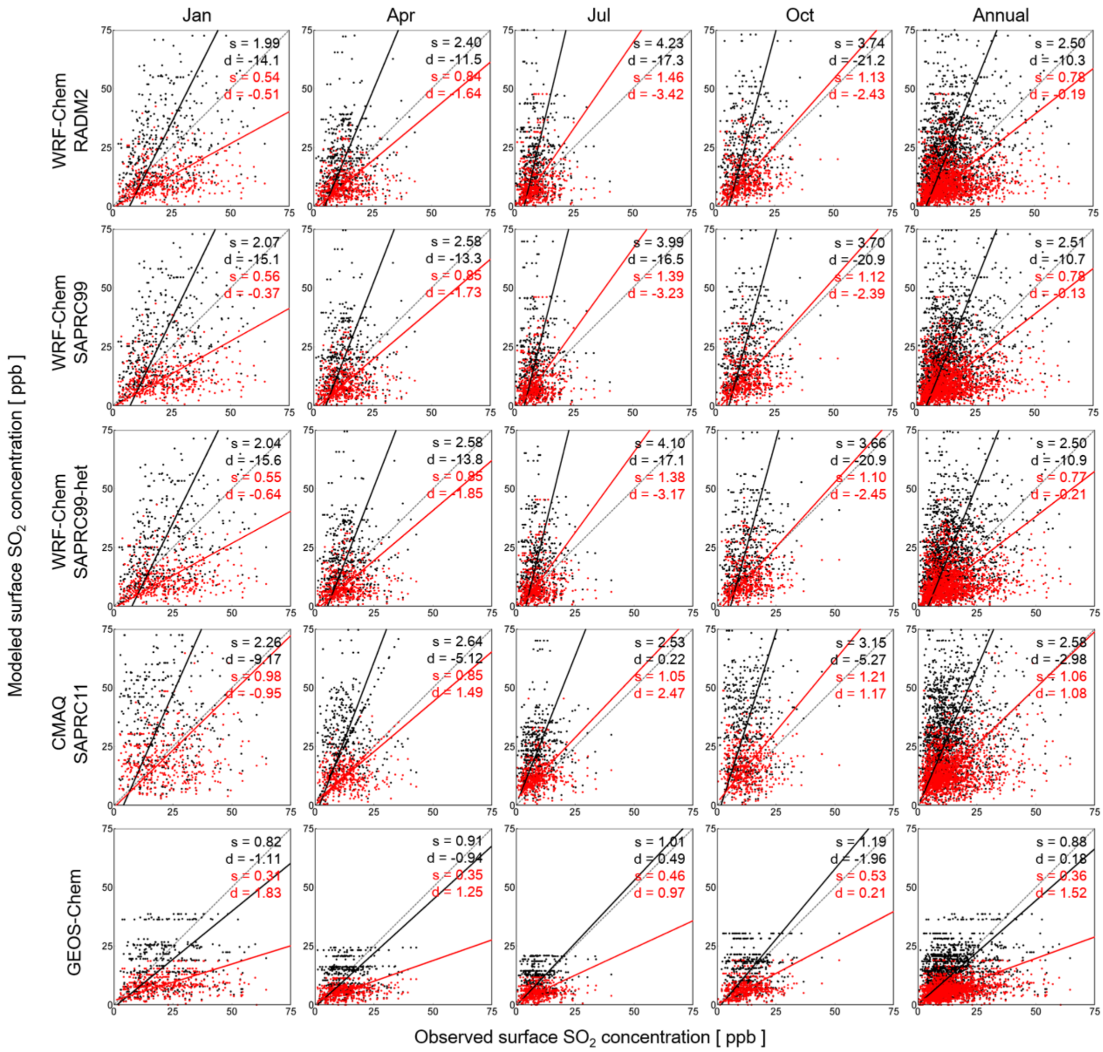

Figure S7. Scatter plot of simulated monthly mean surface SO_2 using prior (black) and posterior (red) emissions versus surface observations for January, April, July and October 2009. The slope (s) and intercept (d) of each trend line are also shown.

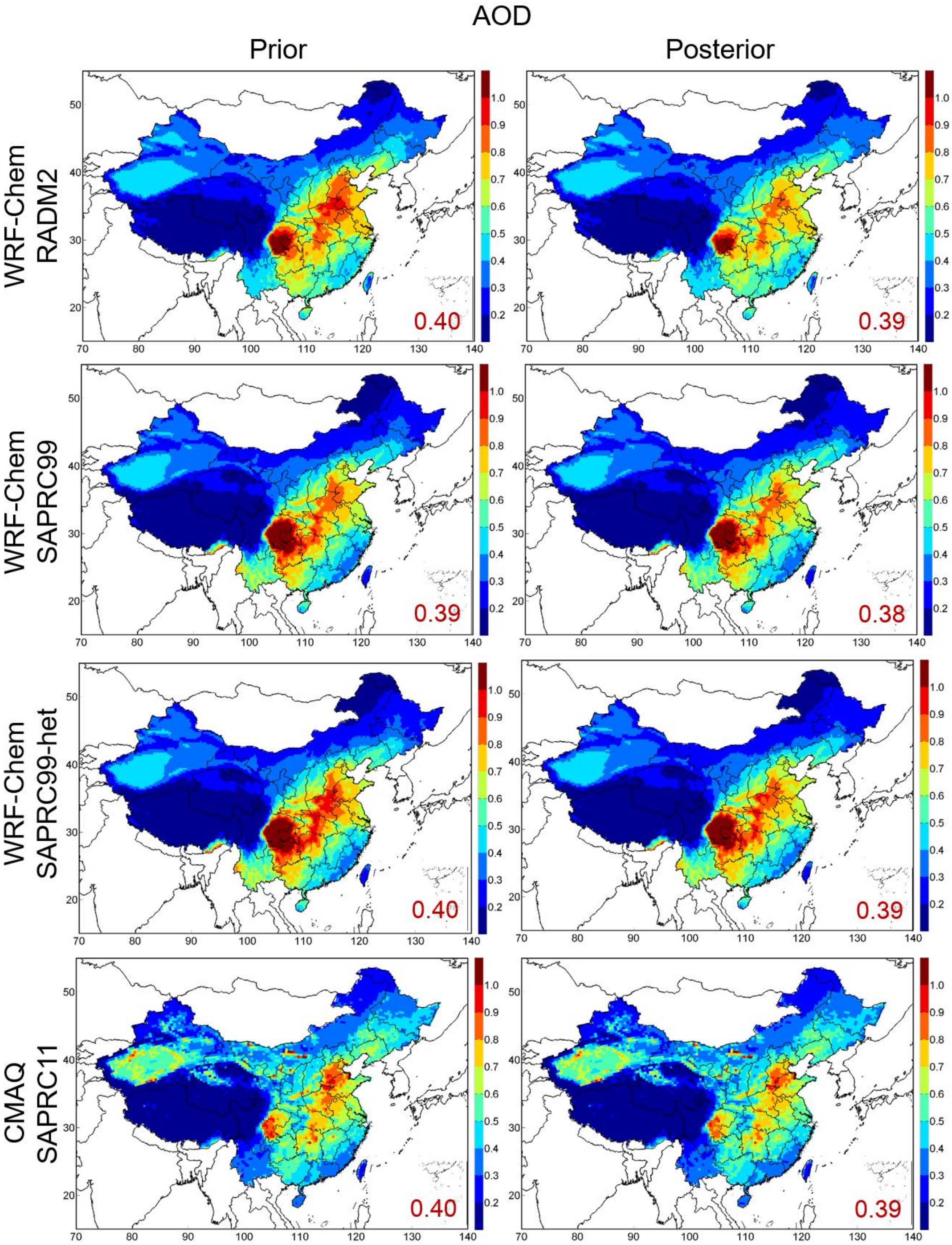

Figure S8. Annual AOD in China averaged for 2009. The left and right columns are from prior and posterior simulations using different models and mechanisms, respectively.

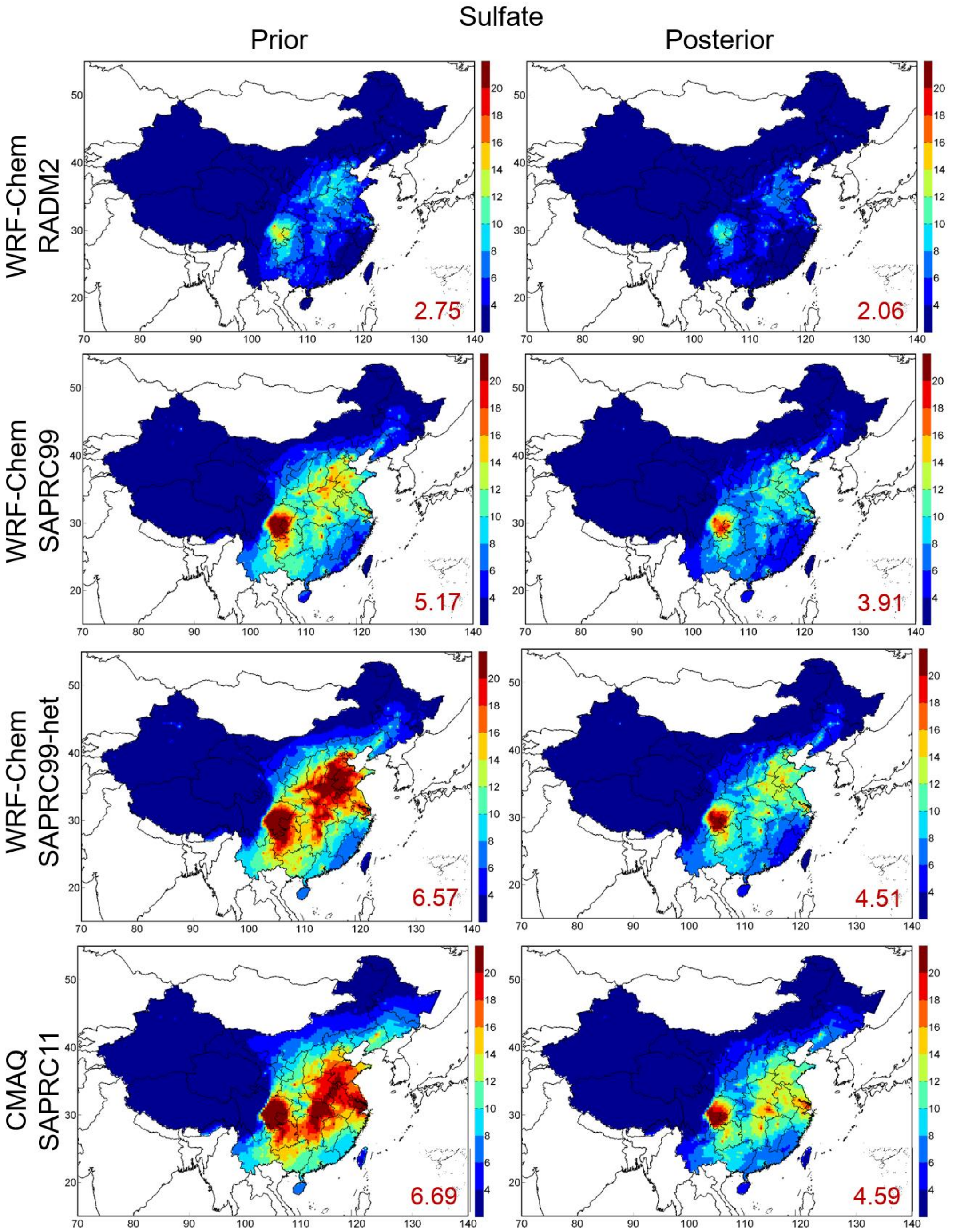

Figure S9. Simulated monthly surface sulfate (□g m^{-3}) in China averaged for 2009 using different models and mechanisms. The left and right are from prior and posterior simulations, respectively.

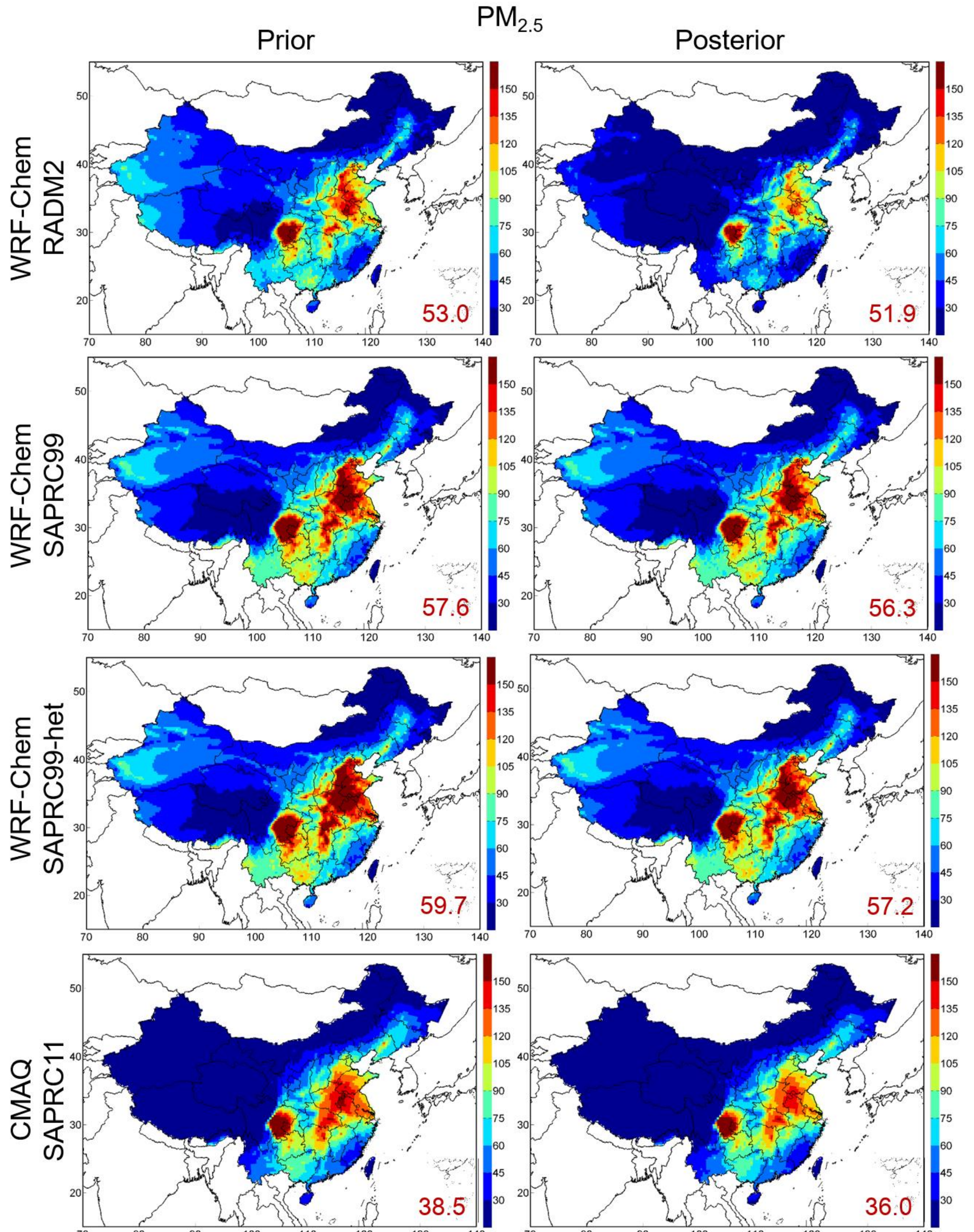

Figure S10. Simulated monthly surface $PM_{2.5}$ (□g m^{-3}) in China averaged for 2009 using different models and mechanisms. The left and right are from prior and posterior simulations, respectively.

Reference

Binkowski, F.S. and S.J. Roselle (2003), Models-3 Community Multiscale Air Quality (CMAQ) model aerosol component: 1. Model description, J. Geophys. Res., 108(D6), 4183, doi:10.1029/2001JD001409.

Carlton, A.G., P.V. Bhave, S.L. Napelenok, E.O. Edney, G. Sarwar, R.W. Pinder, G.A. Pouliot, M. Houyoux, 2010: Model Representation of Secondary Organic Aeros ol in CMAQv4.7. *Env. Sci. & Techno.* 44 (22), 8553-8560.

Carter, W.P.L. (2000a), Documentation of the SAPRC-99 Chemical Mechanism for VOC Reactivity Assessment. Report to the California Air Resources Board, Contracts 92e329 and 95e308.

Carter, W.P.L. (2000b), Implementation of the SAPRC-99 Chemical Mechanism into the Models-3 Framework. Report to the United States Environmental Protection Agency.

Carter, W.P.L. and G. Heo (2012), Development of revised SAPRC aromatics mechanisms. Final Report to the California Air Resources Board, Contracts No. 07-730 and 08-326.

Easter, R.C., S.J. Chan, Y. Zhang, R.D. Saylor, E.G. Chapman, N.S. Laulainen et al. (2004), MIRAGE: Model description and evaluation of aerosols and trace gases. *J. Geophys. Res.*, 109: D20210. Doi:10.1029/2004JD004571.

Foley, K.M., S.J. Roselle, K.W. Appel, P.V. Bhave, J.E. Pleim, T.L. Otte, et al. (2010), Incremental testing of the Community Multiscale Air Quality (CMAQ) modeling system version 4.7, *Geosci. Model Dev.*, 3, 205–226, doi.org/10.5194/gmd-3-205-2010.

Liu, H., D.J. Jacob, I. Bey, and R.M. Yantosca (2001), Constraints from 210Pb and 7Be on wet deposition and transport in a global three-dimensional chemical tracer model driven by assimilated meteorological fields. *J. Goes. Res.*, 106(D11), 12,109–12,128. 10.1029/2000JD900839

Qu, Z., D. K. Henze, N. Theys, J. Wang, and W. Wang, Hybrid mass balance/4D-Var joint inversion of NOx and SO2 emissions in East Asia, J. Geophys. Res.-Atmosphere, 124, 8203-8224, 2019.

Schell, B., I.J. Ackermann, H. Hass, F.A. Binkowski and A. Ebel (2001), Modeling the formation of secondary organic aerosol within a comp rehensive air quality model system. *J. Geophys. Res.*, 106: 28275-28293, 10.1029/2001JD000384.

Stockwell, W.R., P. Middleton, J.S. Chang, X.Y. Tang (1990), The second generation regional acid deposition model chemical mechanism for regional air quality modeling, *J. Goes. Res.*, 95, 10, 16343-16367.

Wang, G.H., R.Y. Zhang, M.E. Gomez, L.X. Yang, M.L. Zamora et al. (2016), Persistent sulfate formation from London Fog to Chinese haze, *PNAS*, 113, 13630-13635, doi:10.1073/pnas.1616540113.

Wang, Y., D.J. Jacob, and J.A. Logan (1998), Global simulation of tropospheric O3-NOx-hydrocarbon chemistry: 1. Model formulation. *J. Goes. Res.*, 103(D9), 10,713–10,725. 10.1029/98JD00158.

Wesely, M.L. (1989), Parameterization of surface resistances to gaseous dry deposition in regional-scale numerical models. *Atmos. Environ.*, 23(6), 1293–1304. 10.1016/0004-6981(89)90153-4.

Zaveri, R.A., R.C. Easter and A.S. Wexler (2005), A new method for multicomponent activity coefficients of electrolytes in aqueous atmospheric aerosols. *J. Geophys. Res.*, 110: D02201. doi:10.1029/2004JD004681.

Zaveri, R.A., R.C. Easter, J.D. Fast and L.K. Peters (2008), Model for Simulating Aer osol Interactions and Chemistry (MOSAIC), *J. Geophys. Res.*, 113, D13204, 10.1029/2007JD008782.